

## **Development of Ceramic Humidity Sensor for the Korean Next Generation Reactor**

**Na Young Lee, Il Soon Hwang, Chang Rock Song, and Han Ill Yoo**

Seoul National University  
San 56-1, Shinlim-dong, Kwanak-gu, Seoul 151-742, Korea

**Sang Duk Park and Jun Seog Yang**

Korea Electric Power Research Institute  
103-16 Munji-dong, Yusong-gu, Taejon 305-380, Korea

(Received January 12, 1998)

### **Abstract**

Leak-before-break(LBB) approach has been shown to be both cost effective and risk reductive when applied to high energy piping in nuclear power plants. For the Korean Next Generation Reactor (KNGR) development, LBB application is considered for the Main Steam Line(MSL) piping inside containment. Unlike the primary system leakages, the MSL leak detection systems must be based on principles other than radioactivity measurements. Among humidity, heat and acoustic noise currently being considered as indicators of leakage, we explored humidity as an effective one and developed ceramic-based humidity sensor which can be qualified for LBB applications. The ceramic material, sintered and annealed  $\text{MgCr}_2\text{O}_4\text{-TiO}_2$ , is shown to increase its electrical conductivity drastically upon water vapor adsorption over the entire temperature range of interest. With this ceramic sensor specimen, we suggested installation-inside-the-piping method by which we can detect leakage more rapidly and sensitively. In this paper, we describe the progress in the development and characterization of ceramic humidity sensor for the LBB application to the MSL of KNGR.

### **I. Introduction**

All nuclear power plants designed prior to 1983 were required to take into account the dynamic effects by postulating circumferential and/or longitudinal ruptures in main coolant loop(MCL) and branch line piping[1]. As results,

these primary system pipings were required to be installed with various protective measures such as pipe whip restraints, snubbers, jet deflectors, jet impingement shields, and oversized component supporters[1]. But these protection devices develop the potential for unintended thermoelastic restraints to piping,

the accessibility problems associated with in-service inspection and maintenance, the increased radiation exposure to workers, and the loss of plant thermal output. Furthermore, the protection structures involve components and space that are costly to install and maintain.

Since early 1980's, the U.S. N.R.C. had performed the studies on the possibility of a double-ended guillotine break(DEGB) or equivalent of the primary piping systems. The U.S. N.R.C. formulated the LBB approaches and acceptance criteria which culminated in 1983 by issuing NUREG-1061 Volume 3[2]. From this, various LBB applications were made, on a case by case basis, in the quest for the exemption from the DEGB requirement.

## **2. Review of Leak Detection Systems for LBB Application**

### **2.1. LBB Analysis**

Analysis on LBB applicability begins with fracture mechanics analysis steps in accordance with SRP 3.6.3[5] and NUREG-1061[3]. The first step is a screening against material degradation mechanisms including creep, corrosion, stress corrosion cracking, indirect causes and cleavage. If any of these degradation mechanisms is judged to be operable, the pipe is not eligible for an LBB application. In the second step, pipe loads should be determined as the sum of normal operation and safe shutdown earthquake(SSE) loads. During normal operation, the leak size crack(LSC) is defined as a crack that develops a steady leak rate of 10 gpm (38 l/min). The leak detection system for LBB should be capable of detecting a leak rate of 1 gpm (3.8 l/min) within one hour with an

adequate redundancy and diversity[3]. The final step is the stability evaluation for the LSC based on the pipe loads using elastic-plastic fracture mechanics, generally by J-T method[4].

### **2.2. Leak Detection Systems at Korean Standard Nuclear Power Plants**

According to NUREG-1061, the following criteria must be satisfied with a piping system to be qualified for an LBB application[2,3] ;

- (1) Three independent leak detection systems are required and each with three redundancy should be capable of detecting leakage less than 1 gpm within one hour for the primary system.
- (2) A throughwall leak size crack(LSC) which is large enough to leak 10 gpm must be stable for the postulated pipe load that is equal to root 2 times the sum of the normal operation and SSE loads.
- (3) A throughwall crack twice as long the LSC must be stable under the sum of the normal operation and SSE loads.

As the KNGR design is patterned after that of Korean Standard Nuclear Power Plant (KSNPP), the leak detection system of the KSNPP is considered to be the reference. In Young Gwang Nuclear Unit (YGN) 3&4 that are early versions of KSNPP, several containment parameters are monitored for the detection of primary system leakages. Three essential leakage detection methods include 1)containment atmosphere particulate radioactivity monitoring, 2)containment sump level and flow monitoring, and 3)containment atmosphere gaseous radioactivity monitoring[3]. It is worthwhile to note that these essential detection systems are global sensors monitoring collective leakage from the primary system.

### 2.3. Leak Detection System Requirement for the MSL

Radioactivity-based detection systems, however, can not be applied to main steam line due to extremely low radioactivity level in secondary water during normal operation. It is clear from the first unsuccessful experience with LBB license application for MSL of Ulchin 3&4, the first version of KSNPP, that the requirements for the leak detection technique for the secondary system need to be defined more clearly. Leak detection systems recommended in NUREG 1061 are referred to Reg. Guide 1.45[6]. Since its first publication in 1973, Reg. Guide 1.45 has not been updated although significant progress has been made in both LBB knowledgebase and the leak detection technology. To detect leakage of MSL for LBB application, however, the use of local humidity sensor is begun recently for high sensitivity and for accurate positioning of leak location. The local sensors suggested in Reg. Guide 1.45 are already implemented in European nuclear power plants[17].

On this ground, we define the requirements of the leak sensors for MSL in accordance with NUREG-1061[3], as follows;

- (1) Leak detection system should be able to detect 1 gpm in the identified leak, and 0.1 gpm in the unidentified leak.
- (2) The leak detection systems must have three diversity, each with three redundancy.
- (3) Local sensors as well as global sensors are applicable.

Among the qualified leak detection systems, containment sump level could be used for both MCL and MSL in the case of identified leaks. Therefore at least two additional detection systems are needed to satisfy the diversity

requirements.

### 2.4. Local and Global Humidity Detection Methods

In System 80+, containment air humidity is to be measured for MSL leak detection[2]. Due to large containment air volume, however, the global humidity monitoring techniques have lower sensitivity and slow response. Siemens has developed a local humidity detection method, designated on FLÜS, and installed at both German and Swedish nuclear power plants for LBB purpose[17]. Similarly a local humidity sensor has been explored in this study. For its application in a close proximity to MSL piping, the sensor needs to endure high temperature up to 300°C. After reviewing literatures, we selected  $\text{MgCr}_2\text{O}_4\text{-TiO}_2$  as a promising candidate material. We present the status of the sensor development and the results of characteristic study in this paper.

## 3. Development of the Ceramic Humidity Sensor

### 3.1. Sensor Materials Review

To be applicable inside the main steam line insulation sheath, the sensor should be able to withstand high temperature. For this reason, we choose ceramic materials as candidates and surveyed some ceramic materials which are superior in physical strength and chemical resistance as well as the electrical properties. Among these,  $\text{MgCr}_2\text{O}_4\text{-TiO}_2$  is operable up to 300°C which is well matched with main steam line condition and known to have good sensitivity in this temperature region. We have thus determined to develop  $\text{MgCr}_2\text{O}_4\text{-TiO}_2$  ceramic humidity sensor.

### 3.2. Conduction Mechanism of $\text{MgCr}_2\text{O}_4 - \text{TiO}_2$

The mechanism of surface conduction in  $\text{MgCr}_2\text{O}_4 - \text{TiO}_2$  involves several microprocesses. The migration or diffusion of protons in the chemisorbed monolayer is usually described by the hopping model as the process of discrete jumps of a charge carrier from site to site over an energy barrier. When the first layer of molecules is adsorbed on the surface grains of  $\text{MgCr}_2\text{O}_4 - \text{TiO}_2$  as shown in Fig 1, a dissociative mechanism leads to form a hydroxyl ion and a proton; the former is chemisorbed on a surface metal ion and the latter associates with a surface oxygen atom to form a second hydroxyl ion. Chromium is believed to be the most active surface metal ion since the  $\text{Cr}^{3+}$  ion combines with hydroxyl easily. Weakly bonded hydroxyl groups, then, dissociate to provide mobile protons. The mobile proton on the surface can migrate by the hopping mechanism to increase the electrical conductivity.

At low humidity, physically adsorbed first water layer is localized by double hydrogen bonding which cannot orient with an ac field. As relative humidity increases, however, multilayers are formed on the ceramic surface where water molecules are hydrogen-bonded to form a liquid-like network thereby capacitance is increased. With the increased dielectric constant, dissociation

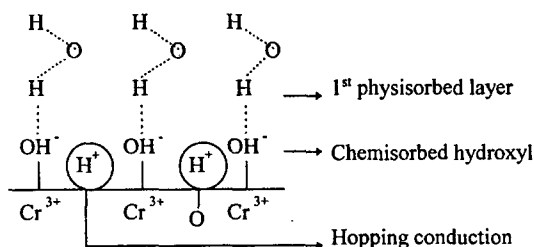


Fig 1. Conduction Mechanism in  $\text{MgCr}_2\text{O}_4 - \text{TiO}_2$

of water into hydromium ( $\text{H}_3\text{O}^+$ ) increases to enhance the ionic conduction[8]. Resultant surface conductivity,  $\sigma_H$ , increases with the humidity due to the combined effect of the proton hopping and the ionic conduction. Hence the total conductivity,  $\sigma$ , is expected to increase with humidity as can be described by Ohm's law;

$$\sigma = \sigma_i + \sigma_H \quad (1)$$

where  $\sigma_i$  is the intrinsic conductivity

$\sigma_H$  is the surface conductivity due to adsorbed carriers

## 4. Experiments

### 4.1. Materials

Raw materials used in preparing the specimens include 99.9% pure  $\text{MgO}$ , 99% pure  $\text{Cr}_2\text{O}_3$ , and 99.9% pure  $\text{TiO}_2$  powder.  $\text{MgCr}_2\text{O}_4 - \text{TiO}_2$  is composed of 70 mol%  $\text{MgCr}_2\text{O}_4$  and 30 mol%  $\text{TiO}_2$ . The raw materials were milled with an alumina ball mill in ethanol for 24 hours. After drying, calcination was carried out at  $1100^\circ\text{C}$  for 10 hours. Then, X-ray diffraction (XRD) was performed with MAC model M18XHF22 XRD analyzer to verify that the calcined material has single phase. After the verification, the powder mixture calcined at  $1100^\circ\text{C}$  was sieved with  $150\ \mu\text{m}$  and  $250\ \mu\text{m}$  sieves in sequence to obtain a powder size range between  $150$  and  $250\ \mu\text{m}$ . Then the powder mixture was pressed into a rectangular block at a pressure of 32 MPa followed by a cold-isostatic pressing (CIP) at a pressure of 100 MPa. The formed  $\text{MgCr}_2\text{O}_4 - \text{TiO}_2$  was sintered at  $1400^\circ\text{C}$  for 10 hours in air. Some of sintered specimens were annealed at  $1100^\circ\text{C}$  for 24 hours in air in order to immobilize unstable electrons[10].

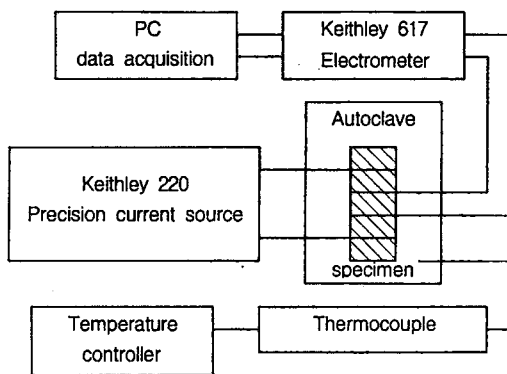


**Fig. 2 Conductivity Measurement Instrument Diagram**

#### 4.2. Conductivity Measurements

A static 1-liter autoclave made of Type 316 stainless steel was used as an environmental chamber for temperature and humidity control. The specimen was a rectangular block with about 1.6 mm by 5.5 mm cross-section and 20 mm length. Overall measurement system is described in Fig. 2. Four-probe DC resistance measurement method was employed by using Ni wires for both current supply and the potential measurement. Lead wires were tied around the cross-section to ensure contacts at all four corners. The spacing between current leads were about 13 mm and that of potential probes was 9 mm. Keithley model 220 current source and Keithley model 617 electrometer were used for the DC resistance measurement as a part of a fully computerized experiment system. The autoclave was preheated and evacuated by mechanical vacuum pump to remove possible humidity in atmosphere and also to facilitate the rapid introduction of test water. Then the autoclave temperature was stabilized to a desired test condition. Controlled amount of water was then inserted through a micropipette and micrometering valve to achieve the desired humidity. The potential drop was measured with

time at a constant current in the range between  $10^{-6}$  and  $10^{-9}$  ampere.

## 5. Results and Discussion

### 5.1. Results

Two tests were performed with the annealed specimen initially in dry and then humid air to identify its humidity-response characteristics. It showed that the conductivity in dry condition is much lower than that measured in humid condition as we expected. It also shows that relaxation time in humid condition is much longer than that in dry condition, which is shown in Fig. 3.

In Fig. 3, in order to compare the apparent response time of both dry and humid conditions,

the term  $1 - \frac{(\sigma_t - \sigma_i)}{(\sigma_f - \sigma_i)}$  is plotted as a function

of time, where  $\sigma_t$  is the conductivity at time  $t$ ,  $\sigma_f$  is the final conductivity and  $\sigma_i$  is the initial conductivity at each experiment. The conductivity in the absence of water is attributed to electronic and ionic conduction in the bulk material, especially hole in this case. But in humid condition, protons released from water molecules and hydromium ions, which are the main charge carriers, can give rise to capacitance effect on the ceramic surface. In general, a proton is slower than a hole, which is assumed to be responsible for the longer relaxation time in humid condition. P-type conductor behavior of  $\text{MgCr}_2\text{O}_4\text{-TiO}_2$  results from the substitution by a small amount of Mg for Ti[8]. Considering the temperature dependence, the conductivity can be expressed as follows[10].

$$\sigma_I = \frac{\sigma_0}{T} \exp\left[-\frac{\Delta E_A}{kT}\right] \quad (2)$$

where  $\sigma_0$  = a constant related with bulk concentration of intrinsic charge carriers

$E_A$  = activation energy

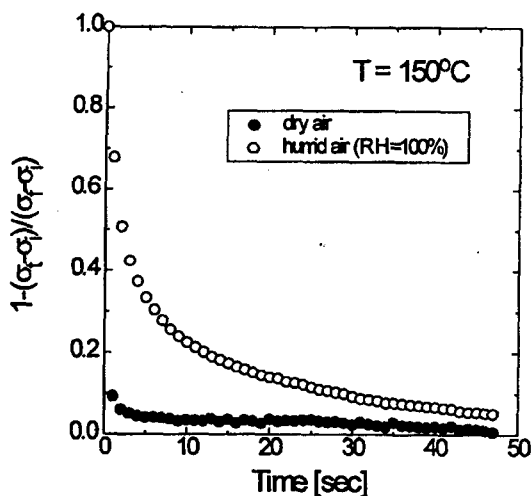


Fig 3. Measured Response of Annealed  $\text{MgCr}_2\text{O}_4\text{-TiO}_2$  with Time at  $150^\circ\text{C}$

Conductivity increase as temperature increases is an intrinsic property of  $\text{MgCr}_2\text{O}_4\text{-TiO}_2$  ceramic material. Figure 4 shows that  $\sigma_i T$  has a linear dependence on  $1/T$ , in agreement with Eq.(2). Conductivity change measured in dry air condition showed difference for each annealed and sintered specimen, which are compared with that of Nitta et al[8]. In this test, the annealed sample showed the lower conductivity and the sintered sample the higher conductivity than that of the sample used by Nitta et. al. This is attributed to the fact that the samples used in this study are sintered at higher temperature than that of Nitta et. al, which is expected to induce more holes. This is evident by the higher conductivity of as-sintered sample. But in the annealed sample, holes are combined with free electrons, explaining its lower conductivity than that of the as-sintered one.

Table 1 compares the apparent activation energy of the samples including Nitta et al[8] in the range of  $100^\circ\text{C}$  to  $300^\circ\text{C}$ .  $\text{MgCr}_2\text{O}_4\text{-TiO}_2$  tested by Nitta et. al. was sintered at  $1360^\circ\text{C}$  and not annealed. Activation energies of both sintered and annealed

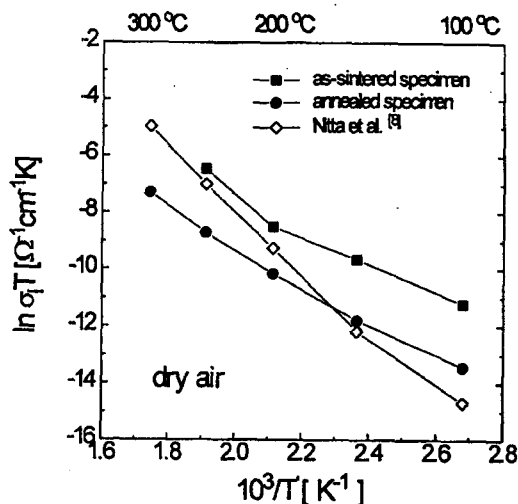
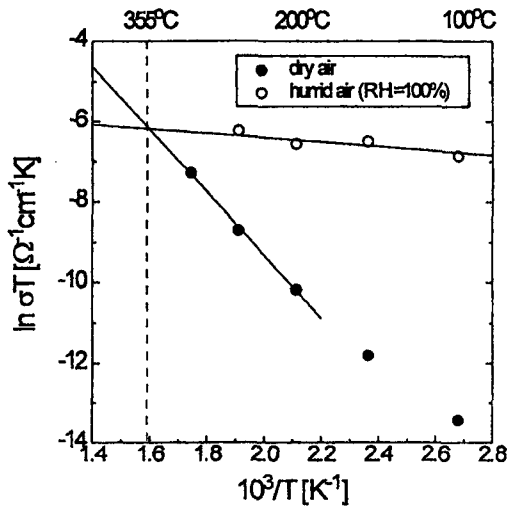


Fig 4. Measured Conductivity of Annealed  $\text{MgCr}_2\text{O}_4\text{-TiO}_2$  in Dry Condition as Function of Temperature

samples are comparable whereas that of Nitta is significantly higher. Then in Fig. 5 we compared the conductivity change in both dry and 100% humid condition as a function of temperature. From this, we can identify that conductivity in dry condition changes more rapidly than in humid condition. It can be explained by the experiment performed by T. Morimoto et. al. which showed that with rising temperature the number of adsorbed water molecules decreases linearly up to  $400^\circ\text{C}$ , and exponentially at higher temperatures[17]. For this reason, the conductivity difference between dry and humid condition is much larger at lower temperature than that at the higher temperature. The extension lines are crossed at about  $355^\circ\text{C}$  that corresponds to the upper temperature limit of our sensor system. Activation energy measured in humid condition is smaller than that in dry air by a factor of ten. For activation energy is the energy needed to generate and transport a hole in this system, sintered and annealed sample should have similar values. But in humid condition, activation energy is small

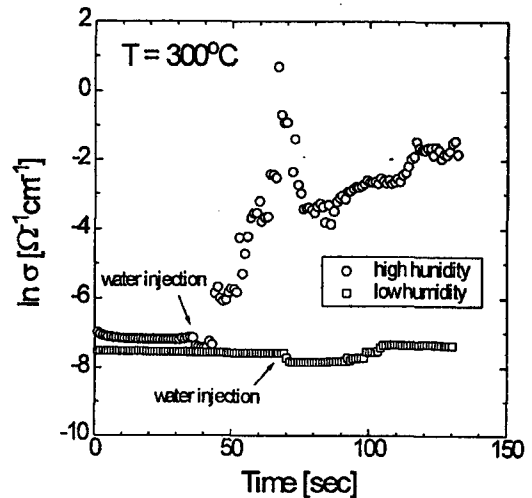
**Table 1. Activation Energy of  $\text{MgCr}_2\text{O}_4\text{-TiO}_2$  in Dry Air at 1 atm**

Test	annealed sample tested in dry air	sintered sample tested in dry air	annealed sample tested in humid air	sintered sample tested in dry air by Nitta[8]
$E_A$ [kJ/mole]	$64.9 \pm 3.1$	$57.9 \pm 12.8$	$5.95 \pm 1.79$	$96.5 \pm 1.10$

**Fig 5. Conductivity Change of Annealed  $\text{MgCr}_2\text{O}_4\text{-TiO}_2$  in Dry and 100% Humid Condition**

because of adsorbed water molecules.

Transient tests were performed with the annealed specimen by injection of controlled amount of water into the evacuated autoclave. To clearly identify humidity response with time, we inserted water after dry air operation for an initial period. Test result is shown in Fig. 6. At high humid condition, conductivity of the ceramic sensor showed a brief dip upon water injection followed by a rapid increase within one minute at 300°C. In low humid condition, it showed a small dip and conductivity increased slightly. It is because in low humidity condition, humidity effect cannot be distinguished from temperature effect for it is supposed that temperature drop by

**Fig 6. Humidity Response vs. Time of Annealed Sample at 300°C**

injection of cold water cannot be neglected.

## 5.2. Discussion on Applicability to MSL

Results showed that  $\text{MgCr}_2\text{O}_4\text{-TiO}_2$  sensor can detect local humidity change at temperature from 25°C to 300°C. In the first stage of adsorption, the conductivity increase of  $\text{MgCr}_2\text{O}_4\text{-TiO}_2$  upon water adsorption is attributed to the production of mobile proton from the chemical bonding between  $\text{Cr}^{3+}$  and  $\text{OH}^-$ [8]. At high humidity, hydromium ions from physisorbed water molecules become the primary charge carrier. MSL of KNGR is operated at 290°C with insulation sheath filled with glassfiber, as shown in Fig 7. Local humidity

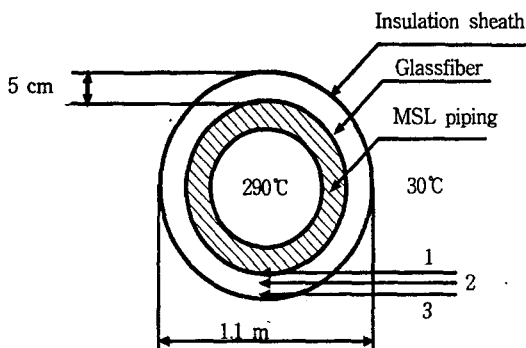


**Fig. 7. Cross-section of the KNGR Main Steam Line**

monitoring around the pipe can be one of very sensitive and rapid method to detect high temperature steam leakage. As the chemisorption is believed to occur at the higher temperature, the sensor reversibility needs to be studied.

If the miniaturized ceramic humidity sensor is installed between the insulation and sheath (position 3), we can detect leak with some delay due to the insulation. The time delay also needs to be determined to ensure that it can meet Reg. Guide 1.45 requirements. The most direct and immediate detection can be made by placing the sensor between the pipe and insulation (position 1) at the expense of more stringent high temperature qualification requirements.

An intermediate sensitivity could be achieved if the sensor is applied within the insulation (position 2). Numerical analysis is to be performed to compare the detection capability and time response at each of the three possible positions.

## 6. Conclusions

Local humidity detection method has been accepted recently for LBB purpose in several European nuclear power plants. For LBB application to MSL of KNGR, a ceramic-based

humidity sensor has been developed as a new local leak detection method with adequate sensitivity over the entire temperature range. The sensor behavior was very reproducible when the ceramic was annealed after sintering. The conductivity-based sensor is shown to respond unequivocally to humidity changes within one minute over 25°C to 300°C. To apply it to main steam lines at KNGR for the LBB, further development including the leak rate quantification method and characterization of time response in the realistic insulated piping environment are in progress.

## Acknowledgment

This work has been financially supported by the Korea Electric Power Research Institute as a part KNGR development programs.

## References

1. Proceedings on Specialist meeting on Leak Before Break in Reactor Piping and Vessels, EDF - FRAMATOME - CEA - EC DGXI Nuclear Electric - OECD - IAEA - NRC - SFEN, LYON, FRANCE (1995)
2. Combustion Engineering, Inc, "Applicability of Leak-Before-Break to the Young Gwang 3&4 Main Coolant Loop & Surge Line" (March, 1983)
3. U.S. N.R.C., "Evaluation of Potential for Pipe Breaks", NUREG-1061, Vol 3, (1984)
4. U.S. N.R.C., "Leak-Before-Break Evaluation Procedures", Standard Review Plan 3.6.3, Draft, (1987)
5. P. Jax, "Detecting and locating the smallest leaks early", Nuclear Engineering International, pp. 22-24 (1995)
6. U.S. N.R.C., "Reactor Coolant Pressure Boundary Leakage Detection Systems", Regulatory Guide 1.45, Rev.1 (1982)



7. K. Nii, M. Kuwabara, F. Odahara, Y. Ise, O. Kawasaki, "Development of Portable trace steam leak detection instrument", Kansai Electric Power Cooperation R&D Center, Japan, Comprehensive research summary No. 82-017, (1982)
8. T. Nitta, Z. Terada, and S. Hayakawa, "Humidity-sensitive Electrical Conduction of  $\text{MgCr}_2\text{O}_4\text{-TiO}_2$  Porous Ceramics," J. Am. Ceram. Soc., Vol 63 No[5-6], pp. 295-300 (1980)
9. Y-C Yeh, T-Y Tseng, and D-A Chang, "Electrical Properties of  $\text{TiO}_2\text{-K}_2\text{Ti}_6\text{O}_{13}$  Porous Ceramic Humidity Sensor", J. Am. Ceram. Soc., Vol. 73 No[7] pp. 1992-98 (1990)
10. N. M. Tallan, "Electrical Conductivity in Ceramics and Glass", pp. 37-169, Marcel Dekker, Inc. (1974)
11. T. Nenov and S. Yordanov, "Ceramic sensor device materials", in Sensors and Actuators, B. pp. 117-122, (1992)
12. D. M. Norris, B. Chexal, "PICEP : Pipe Crack Evaluation Program", EPRI Report NP-3596-SR, Rev. 1, Electric Power Research Institute, Palo Alto, CA.(1984)
13. D.J Ayres, J.J. LaRussa, B.R. Ganta, S.C. Austin, "Application of Leak-Before-Break Analysis to PWR Piping Designed by Combustion Engineering", EPRI NP-5010, Electric Power Research Institute, Windsor, Connecticut (1987)
14. Walter J. Moore, "Physical Chemistry, 4th Edition ", Prentice-Hall, Inc. pp. 497-507. (1972)
15. J. H. Anderson and G. A. Parks, "The electrical conductivity of Silica Gel in the Presence of Adsorbed Water," J. Phys. Chem., Vol.72 No.[10] pp. 3662-3668 (1968)
16. J. H. Park, M.S. Thesis, Division of Materials Science and Engineering, Seoul National University (1989)
17. T. Morimoto, M. Nagao and F. Tokuda, "The relation between the amounts of chemisorbed and physisorbed water on metal oxides", J. Phys. Chem., 73 pp. 243-248 (1969)
18. S. S. Pingale, S. F. Patil, M. P. Vinod, G. Pathak, K. Vijayamohanan, "Mechanism of humidity sensing of Ti-doped  $\text{MgCr}_2\text{O}_4$  ceramics", Materials Chemistry and physics, 46 pp. 72-76 (1996)